Materials Chemistry and Physics 121 (2010) 154–160

Contents lists available at ScienceDirect

Materials Chemistry and Physics

journal homepage: www.elsevier.com/locate/matchemphys

On the magnetic and dielectric properties of nickel–neoprene nanocomposites

E. Muhammad Abdul Jamal [a], P.A. Joy [b], Philip Kurian [c], M.R. Anantharaman [a,*]

[a] Department of Physics, Cochin University of Science and Technology, Cochin, India
[b] National Chemical Laboratory, Pune, India
[c] Department of Polymer Science and Rubber Technology, Cochin University of Science and Technology, Cochin, India

ARTICLE INFO

Article history:
Received 15 January 2009
Received in revised form 25 October 2009
Accepted 3 January 2010

Keywords:
Composite materials
Dielectric properties
Magnetic properties
Elastomers

ABSTRACT

Nickel nanocomposites were prepared by incorporating nickel nanoparticles in a neoprene matrix according to a specific recipe for various loadings of nickel particles. The dielectric properties of these composites were evaluated for different frequencies ranging from 100 kHz to 8 MHz at different temperatures from 30 °C to 120 °C. The dielectric permittivity increases with increase of nickel concentration. Increase in temperature enhances the permittivity initially, till 40 °C and thereafter the permittivity decreases. The dielectric loss exhibits relaxation peaks and the peaks shift to lower frequencies with increase in volume fraction of the nickel nanoparticles in the matrix. The evaluation of magnetic and dielectric properties of these composites suggests that the dielectric permittivity can be tailored by an appropriate loading of the filler using semi-empirical equations and the magnetic properties vary according to simple mixture equations.

1. Introduction

The physical properties of polymer materials can be modified by incorporating different types of fillers in the matrix and the resulting composites are suitable for various technological applications [1–4]. The electrical and magnetic properties of the polymeric host can be improved considerably by impregnating magnetic fillers into the matrix [5,6]. Even though magnetic ferrite particles are the commonly employed fillers in such composites, it is possible to prepare magnetic polymer composites by incorporating ferromagnetic metal nanoparticles in polymeric matrix [7]. Nickel is an important ferromagnetic material and magnetic nanocomposites can be prepared by incorporating nickel nanoparticles in a polymer matrix. Neoprene is a commonly available inexpensive synthetic rubber with superlative properties compared to natural rubber as it offers better resistance to weathering, flame and to corrosive chemicals and magnetic composites of neoprene can find applications as electromagnetic interference shielding devices [8]. Ferrite filled neoprene composites were already prepared and characterized by some researchers [9]. Nickel as a filler can alter the dielectric properties of neoprene, since they are metallic inclusions and at the same time, being ferromagnetic can impart high magnetic permeability to the composite and the mouldability of neoprene can give high degree of freedom in terms of shape and size. Magnetic dielectric materials are employed as radiation absorbers and the frequency at which the absorption is most efficient is determined by the magnetic as well as the dielectric properties of these materials [10].

There are several factors which influence the dielectric properties of an elastomer–metal composite. The volume fraction of the filler and the size of the particles play vital roles in deciding its overall electrical property. It is known that these composites display excellent dielectric properties when the volume fraction of the filler is relatively small and a sharp increase in conductivity is noticed beyond a certain threshold loading of the filler [11]. This is because of the formation of conductive paths at and beyond the percolation threshold of the filler particles. However below the percolation threshold, these composites behave as good insulators and their dielectric properties can be tuned by an appropriate loading of the filler. Nanosized nickel particles can thus serve as ideal fillers for tuning the magnetic as well as the dielectric properties of the polymer matrix because they when incorporated in a neoprene matrix not only modify the dielectric properties but also alter the magnetic property of the matrix. Simple semi-empirical relationships can be employed to tailor the dielectric properties of these composites. Various mathematical models are available and it would be appropriate to evaluate which one fits the best of the observed values. For this, knowledge of the dielectric properties of the filler and the matrix are essential at the desired frequency and temperature. The evaluation of the magnetic property and predicting the mass-magnetization values of the composites using simple mixture equation will also enable to tailor the magnetic property of the composite.

* Corresponding author. Tel.: +91 484 2577200/2577404; fax: +91 484 2577595.
E-mail addresses: mraiyer@yahoo.com, mra@cusat.ac.in (M.R. Anantharaman).

0254-0584/$ – see front matter © 2010 Elsevier B.V. All rights reserved.
doi:10.1016/j.matchemphys.2010.01.006

In an earlier article published by the same authors the magnetic and dielectric properties of nickel–natural-rubber composites were investigated [12]. In the present investigation, nickel–neoprene nanocomposites were prepared for various loadings of nickel according to a specific recipe and the dielectric and magnetic properties were evaluated. We will also examine the veracity of the simple semi-empirical relationships in order to predict the properties of these composite materials.

2. Experimental details

2.1. Preparation and characterization of nickel nanoparticles

Nickel nanoparticles lying in the size range of 25–40 nm were prepared by means of a modified sol–gel combustion process developed by the authors, which is under the process of patenting [Patent application 1982/2006 Indian patent]. 0.1 mol of nickel nitrate hexahydrate was dissolved in 20 ml of ethylene glycol and the resulting solution in a beaker was heated by placing it on a hot-plate kept at a temperature of 350 °C. Combustion of the reagents takes place and the resulting spongy material in the beaker is found to be highly porous metallic nickel. Nickel nanoparticles were prepared by grinding this nickel sponge in a mortar and subsequent high energy ball-milling for 2 h in toluene medium. Nanoparticles of nickel were prepared in batches and were thoroughly homogenized later on before using them in the synthesis of nickel–neoprene nanocomposites. The nickel nanoparticles were characterized by X-ray diffractometry (XRD) using Rigaku Dmax X-ray diffractometer for the evaluation of the structural properties. The magnetic properties of the nickel particles were determined using a SQUID magnetometer (MPMS-5S XL Quantum Design magnetomer). Transmission electron microscopy (TEM) was employed to determine the size of the particles using a PHILIPS CM200 electron microscope operating at 20–200 kV having a resolution of 2.4 Å.

2.2. Preparation and characterization of nickel–neoprene composites

Pre-characterized nickel particles were used for the preparation of the composites by incorporating nickel powder in neoprene rubber (W grade) according to a specific recipe [9]. Five sets of composites were prepared with volume fractions of nickel particles in the composite ranging from 0.028 to 0.14.along with a sample of blank neoprene as control sample. Volume fractions of nickel in the composites were calculated by assuming the reported density of cured neoprene (1250 kg m^{-3}) and that of nickel (8912 kg m^{-3}) [13,14]. Neoprene compounds were cured and compression-moulded into sheets of about 2 mm thick using an electrically heated hydraulic press having 45 cm × 45 cm platens at a pressure of 140 kg cm^{-2} in a standard mould after evaluating the cure times for each composite sample separately using a rubber processor analyzer (RPA2000 of α-Technology) at 160 °C. The structural parameters of the composite were evaluated by means of X-ray diffractometry. The magnetic hysteresis studies were done on an EG&G PAR 2000 vibrating sample magnetometer at room temperature. The morphology of the samples was investigated by means of scanning electron microscopy (SEM) (JEOL model JSM – 6390LV)

For dielectric studies, circular discs having a diameter of 12 mm were cut out from the sheets. Dielectric permittivity was evaluated with an HP impedance analyzer (model 4285A) in the frequency range of 100 kHz to 8 MHz at temperatures varying from 30 °C to 120 °C. The samples were inserted between two identical copper discs to form a capacitor in a home-made dielectric cell whose fabrication details were reported elsewhere [15]. The capacitance and the loss tangent were recorded at intervals of 100 kHz using an automated measurement set-up interfaced with a personal computer through a GPIB cable IEE488 with the help of a commercial interfacing and automation software named LabVIEW with the program for data acquisition written in language G which is a graphical programming language much suitable for data acquisition applications. The dielectric permittivity of the sample was calculated using the relation.

$$\varepsilon' = \frac{cd}{\varepsilon_o A} \tag{1}$$

and the dielectric loss by the relation

$$\varepsilon'' = \varepsilon' \tan\delta \tag{2}$$

where c is the capacitance, d is the thickness and A is the area of the composite material inside the copper plates, ε_o is the permittivity of free space, ε' and ε'' are the real and imaginary parts of the complex permittivity of the medium and δ is the loss angle.

3. Results and discussion

3.1. Properties of nickel particles

The XRD pattern of nickel particles is depicted in Fig. 1 and they reveal that crystalline nickel particles with fcc structure were formed without any impurities on comparing the results with published JCPDS data (JCPDS file no. 03-1051). The size distribution of the particles was determined using the Debey–Scherer formula which gives the average particle size (D) of powder sample in terms of the wavelength λ of the X-ray source, the full width at half maximum (β) of the diffraction peak and the angle of diffraction (2θ), in the form [16]

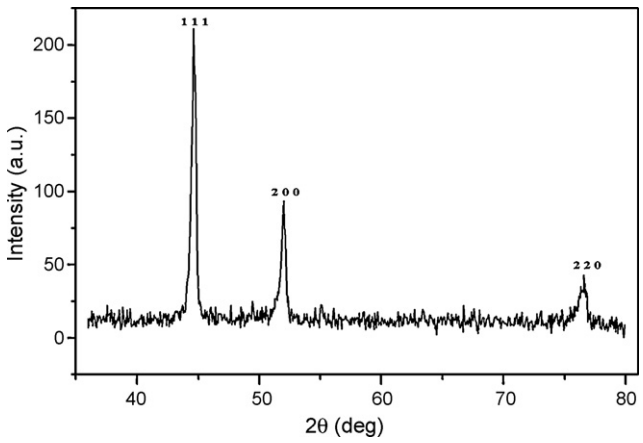

Fig. 1. XRD pattern of nickel particles.

$$D = \frac{0.9\lambda}{\beta \cos\theta} \tag{3}$$

and it was found that the average particle size of the particles is 26 nm. TEM micrograph of the composite (Fig. 2) shows nickel particles in the size range of 25–40 nm validating particle size obtained by the analysis of XRD pattern. A mass-magnetization study of pure nickel was carried out in a SQUID magnetometer and the hysteresis behaviour of the sample is shown in Fig. 3. Ferromagnetic nature of the particles is evident from the hysteresis curve and the saturation mass-magnetization is found to be 47.5 emu g^{-1} and this is consistent with previous reports [17].

3.2. Initial characterization of the composites

Nickel–neoprene composites were synthesized according to a well established curing process reported elsewhere [9]. The XRD patterns of the composite samples with volume fraction of nickel content from 0 (blank neoprene) to 0.28 are shown in Fig. 4. Peaks of unreacted curing agents are visible in the XRD of blank neoprene and are indicated by numbers 1–5. The broad and shallow peak centered at 22° of 2θ, visible in the XRD pattern of blank neoprene is due to the short range ordering of polymer molecules and this kind of peaks is characteristic to rubber samples. But all these peaks visible in the blank sample disappear in the XRD patterns of the composites as nickel becomes the predominant crystalline phase. The diffraction peaks corresponding to that of nickel seen in the composite samples indicate that the nickel is retained in the composites without any structural modifications. Trace amounts of nickel oxide in the form of NiO are evident in the XRD and this might have been formed during the heat treatment of the composites at the time of curing or due to the heat generated while mixing the ingredients. But the content of oxides is insignificantly small (diffraction peaks of NiO are marked with circles). The SEM image shown in Fig. 5 clearly points to the dispersion of nickel particles in the matrix. The magnetic hysteresis of the composites is presented in Fig. 6 and it was observed that their magnetic behaviour is purely ferromagnetic and the observed saturation mass-magnetization of each sample from the graph shows small drops compared to the mass-magnetization calculated from

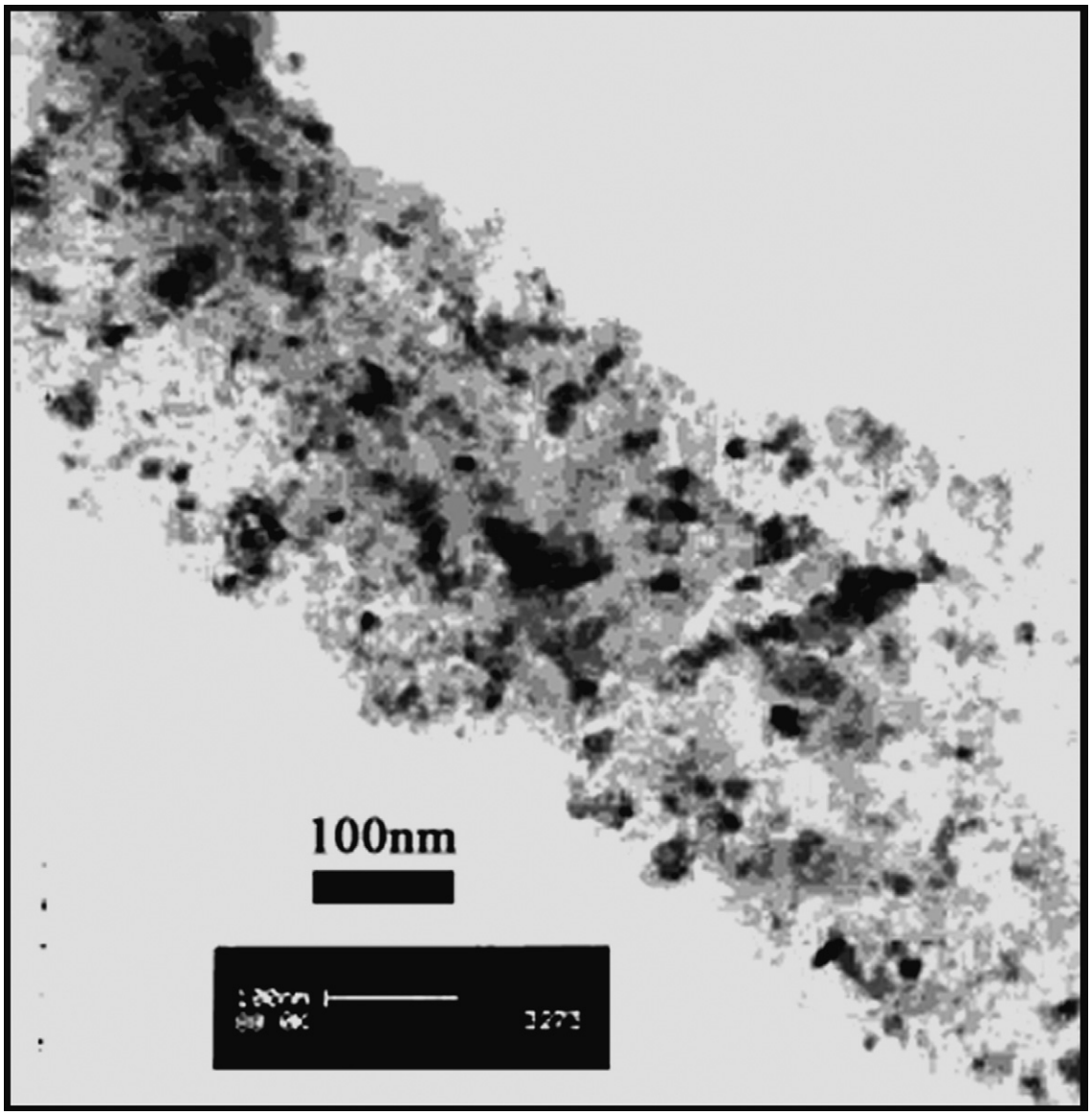

Fig. 2. Transmission electron micrograph of nickel particles.

the actual content of ferromagnetic nickel particles in the samples using the relation

$$M_s(\text{composite}) = \frac{M_s(\text{nickel}) \times m_2}{m_1} \quad (4)$$

where M_s(composite) is the saturation mass-magnetization of the composite, M_s(nickel) is that of nickel particles, m_1 is the total mass of a given sample of composite and m_2 is the mass of nickel particles in this sample. This small drop observed in mass-magnetization can be attributed to the formation of nickel oxide and loss of nickel particles during the process of mixing and curing. The difference in mass-magnetization can also be due to the demagnetization effects caused by the shape of the samples or it might be a combined effect of all the factors mentioned above. The observed and the calculated values of saturation mass-magnetization are tabulated (Table 1) for the sake of comparison.

3.3. Dielectric studies on the composites

Dielectric permittivity and dielectric loss tangent of the composites in the frequency range of 100 kHz to 8 MHz from 30 °C to

Table 1
Observed and calculated saturation mass-magnetization of the composites.

Volume fraction of nickel	Mass of nickel particle in 100 g of neoprene (g)	Total mass of the sample (nickel + neoprene + curing agents) (g)	Calculated mass-magnetization of the sample (emu g^{-1})	Observed mass-magnetization of the sample (emu g^{-1})
0.028	20	130.5	7.18	6.51
0.056	40	150.5	12.47	11.91
0.084	60	170.5	16.54	14.68
0.112	80	190.5	19.76	16.69
0.140	100	210.5	22.37	20.24

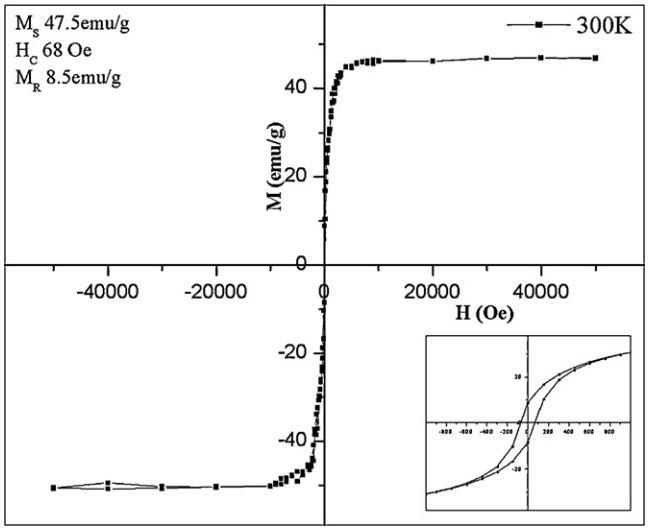

Fig. 3. Magnetic hysteresis graph of nickel particles. The central portion of the graph is shown in the inset.

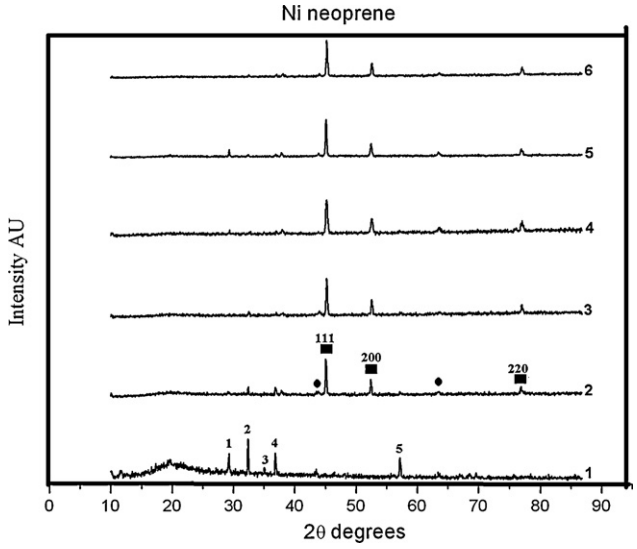

Fig. 4. The XRD patterns of nickel–neoprene composites with volume fraction of nickel 0, 0.028, 0.056, 0.084, 0.112 and 0.140 in steps of 0.028 (graphs numbered from 1 to 6 respectively). The diffraction peaks of unreacted curing agents are marked by numbers 1 to 5. Diffraction peaks of metallic nickel are marked by squares and marked with circles are the diffraction peaks of NiO.

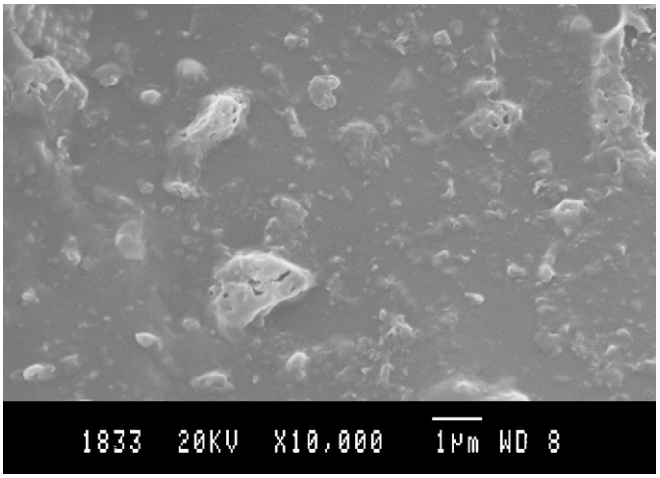

Fig. 5. SEM picture of composite (sample with volume fraction 0.084).

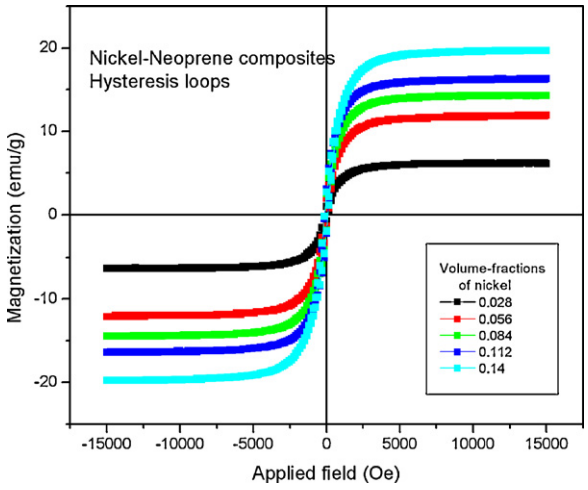

Fig. 6. Magnetic hysteresis of composites recorded at room temperature. The saturation mass-magnetization increases with increase in the concentration of nickel in the composites.

120 °C were determined. All samples including the blank neoprene sample exhibit a steady decrease in dielectric permittivity with the increase of frequency as observed in Fig. 7. Here the composite with 0.084 volume fraction of nickel is taken as a representative sample for depicting the variations since all samples show exactly same kind of behaviour. Neoprene has high permittivity compared to other polymer materials due to the polar nature of its molecules [8]. The decrease in dielectric permittivity with frequency suggests the presence of interfacial polarization in the composite caused by the accumulation of charges at the interfaces of its different components. [18]. Even in blank neoprene the material is granular in nature, providing large amount of grains and grain boundaries and charge accumulation at these interfaces could be the cause of interfacial polarization. Fig. 8 shows the variation of dielectric loss with frequency. Here also the sample of volume fraction 0.084 is shown as a representative sample. At temperatures 30 °C and 40 °C a broad relaxation process is observed in the frequency range. But the broad peak disappears at higher temperatures and at 80 °C, 100 °C and 120 °C the dielectric loss decreases with frequency in the given frequency range. It can be concluded that the broad peak shifts to the

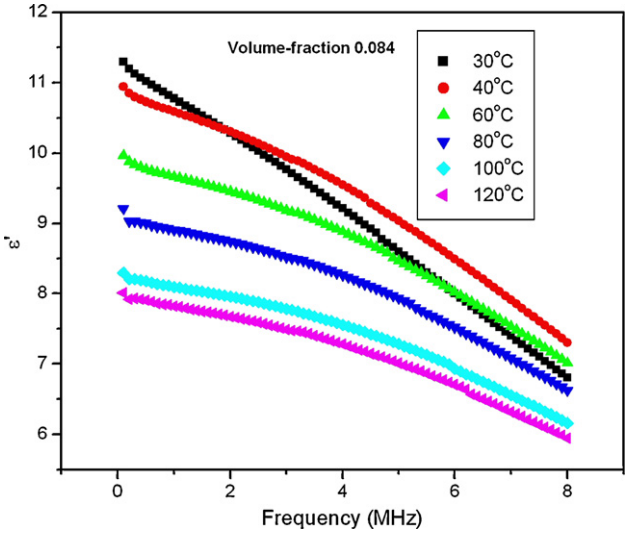

Fig. 7. Variation of dielectric permittivity with applied frequency at temperatures varying from 30 °C to 120 °C.

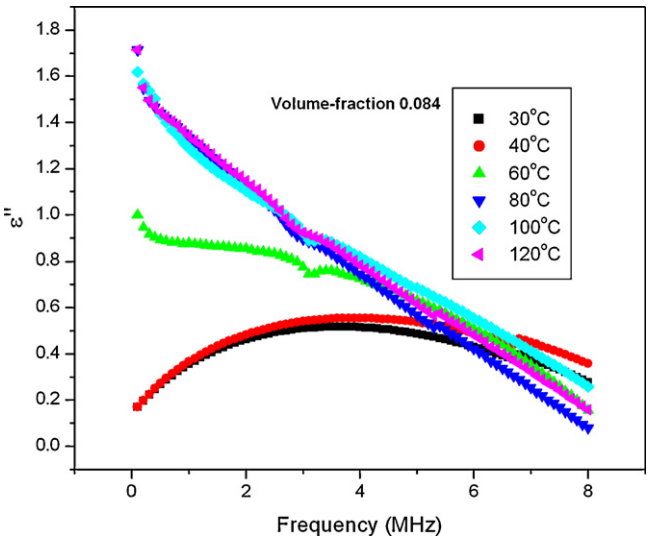

Fig. 8. Variation of dielectric loss with applied frequency at temperatures varying from 30 °C to 120 °C.

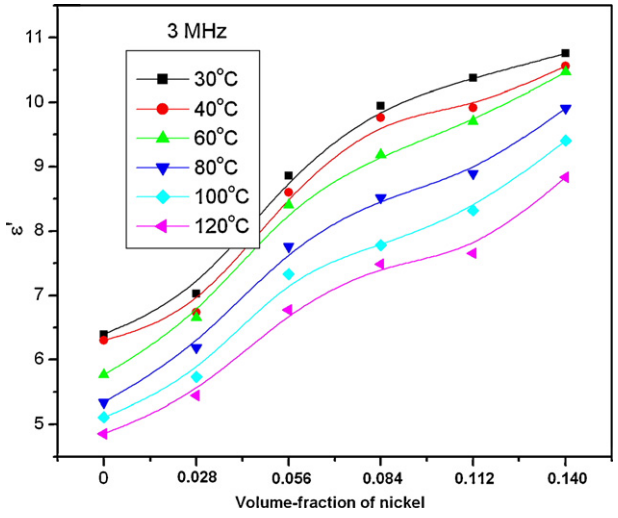

Fig. 9. Variation of the real part of permittivity with nickel content in the composites at a frequency of 3 MHz.

low frequency side as temperature increases. The reason for which is not understood.

It was found that the dielectric permittivity increased with increase of nickel concentration in the matrix at all frequencies as shown in Fig. 9, which is the plot for 3 MHz. The increase in permittivity with increase in filler loading can be understood on the basis of two possible reasons. They are the increase in interfacial area in the composite and the resulting enhancement in the interfacial polarization and the increase in the conductivity of the sample due to the presence of metallic fillers. Enhancement of dielectric permittivity can also be due to the development of internal barrier layer capacitance (IBLC) in the composites, but IBLC usually causes very high permittivity (of the order of 1000) and this does not appear to be a reason for enhancement of permittivity in elastomer composites [19]. It is quite evident that the dielectric permittivity of these materials can be varied by means of varying the filler contents. Many researchers have attempted to interpret the enhancement in dielectric permittivity in metal filled composites and a number of mathematical formulae had been suggested which can be employed to determine the effective permittivity of a composite material [20]. Maxwell–Wagner formula is one such formula which can be employed in the two component system.

$$\varepsilon^* = \varepsilon_1 \frac{2\varepsilon_1 + \varepsilon_2 + 2y(\varepsilon_2 - \varepsilon_1)}{2\varepsilon_1 + \varepsilon_2 - y(\varepsilon_2 - \varepsilon_1)} \tag{5}$$

where ε^* is the dielectric permittivity of the composite and ε_1 and ε_2 are the dielectric permittivity of the two component materials and y is the volume fraction of the filler in a continuous matrix. But we are considering the case metal filled composites and the permittivity of metal is not defined. By assuming the permittivity of metal particles to be very high (nearly infinity) and y is small, Eq. (5) can be reduced to the form [20]

$$\varepsilon^* = \varepsilon_1(1 + 3y) \tag{6}$$

Bruggman had modified this equation to the form (again by considering y is small and neglecting the higher powers of y)

$$\varepsilon = \frac{\varepsilon_1}{(1-y)^3} \tag{7}$$

Beziard et al. proposed another empirical relation based on experimental results in the form [21]

$$\varepsilon^* = \varepsilon_1(1+y)^5 \tag{8}$$

After fitting these models given by Eqs. (6)–(8) we have found that the formula given by Eq. (8) gives better agreement with the experimental results in nickel–neoprene nanocomposites as observed in Fig. 10 where the observed values of permittivity at 3 MHz of applied frequency at various temperatures are compared with those calculated according to Eq. (8). In all the above discussions it is assumed that the mixture of the matrix material with the filler is purely physical and no chemical interactions take place between the filler and the matrix material. Volume fractions were calculated by assuming the density of neoprene to be 1250 kg m^{-3} and that of nickel is 8912 kg m^{-3}. Neoprene sample without filler was prepared for the purpose of comparative study in the same chemical process for the composites and permittivity of this sample also was determined along with the composite samples which were used in model fitting calculations.

The variation of dielectric loss with frequency is plotted for all the samples at room temperature in Fig. 11. It can be observed that, for blank sample, at room temperature (30 °C) the maximum of the dielectric loss is achieved at about 6 MHz and frequency corresponding to the maximum loss is being shifted to the lower side progressively for other samples with increasing content of nickel particles. The dielectric relaxation process is affected by the incorporation of metallic fillers in the elastomeric matrix. The behaviour of the dielectric constant of materials with a single relaxation mechanism can be represented by Debye equations of the form

$$\varepsilon^*(\omega) - \varepsilon_\alpha = \frac{\varepsilon_s - \varepsilon_\alpha}{1 + i\omega\tau} \tag{9}$$

where $\varepsilon^*(\omega)$ is the complex permittivity at angular frequency ω and ε_α is the permittivity at optical frequencies [22]. Eq. (9) can be separated into real and imaginary parts as

$$\varepsilon'(\omega) = \varepsilon_\alpha + \frac{\varepsilon_s - \varepsilon_\alpha}{1 + \omega^2\tau^2} \tag{10}$$

and

$$\varepsilon''(\omega) = (\varepsilon_s - \varepsilon_\alpha)\frac{\omega\tau}{1 + \omega^2\tau^2} \tag{11}$$

The value of ε_α can be considered equal to the value of dielectric constant at optical frequencies where ε_α remains steady and the value of ε_s can be determined by extrapolating the dielectric dispersion curve to lower frequencies. In Eq. (11) the quantity $\varepsilon_s - \varepsilon_\alpha$ is a constant for a given material and the variation of dielectric loss depends on the relaxation time and the frequency only. From Eq. (11) the relaxation time can be calculated taking into account the

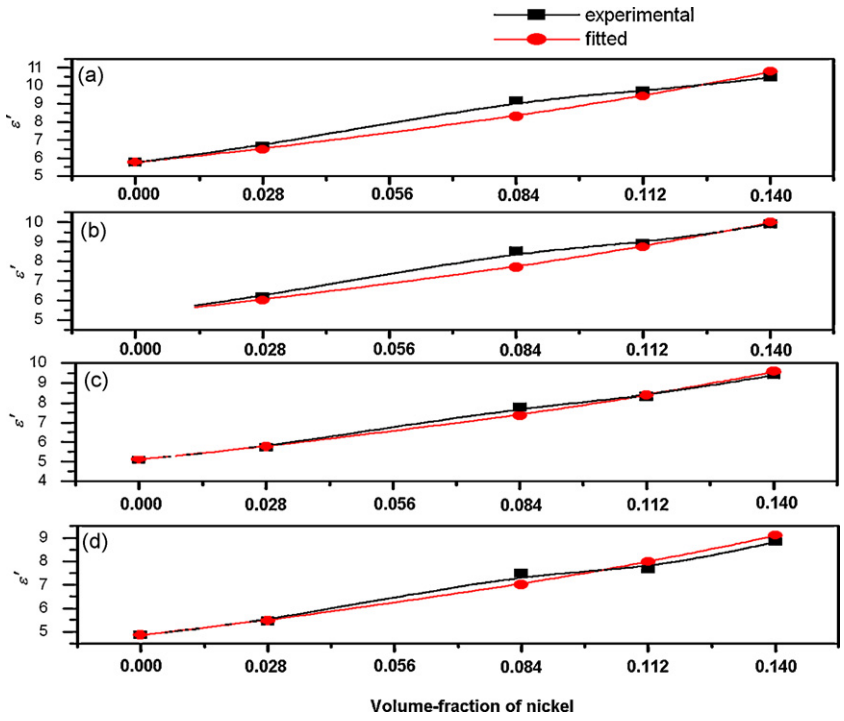

Fig. 10. The observed and calculated variation in the permittivity (at 3 MHz) with the volume fraction of nickel particles in the composites at temperatures 40 °C (a), 60 °C (b), 80 °C (c) and 100 °C (d)

peak of the dielectric loss $d\varepsilon''/d\omega$ vanishes when ε'' is maximum and it can be shown that this happens when $\omega\tau = 1$. For blank neoprene sample without any loading we have obtained a peak in the loss-frequency graph nearly at 6 MHz and the estimated relaxation time from this is 2.65×10^{-8} s. The inclusion of metallic fillers increases the relaxation time of samples, and the peaks get shifted towards the low frequency side progressively as observed in Fig. 9. The 0.112 volume-fraction sample shows a relaxation peak at 4 MHz and for the 0.14 volume-fraction sample the peak is shifted to the position of 2.5 MHz. Increase in filler loading increases the interfacial area inside the composites and accumulation and removal of charges on the interfaces, caused by the applied field, take more time to complete and will lag behind the applied field. The glass transition temperature of neoprene is at −50 °C [13]. Therefore the observed shift in the peaks in the loss-frequency graphs towards the lower frequency side with increase in filler content is a clear indication for the presence of interfacial polarization suggested by the Maxwell–Wagner theory in metal filled polymer samples. But the reason for not observing the relaxation at higher temperatures is not understood.

The effect of temperature on the dielectric permittivity of nickel–neoprene composites is depicted in Fig. 12. The variation of dielectric permittivity of 0.084 volume-fraction sample is shown here as a representative example.

The dielectric permittivity decreases in general with increase in temperature. But at higher frequencies it is observed that

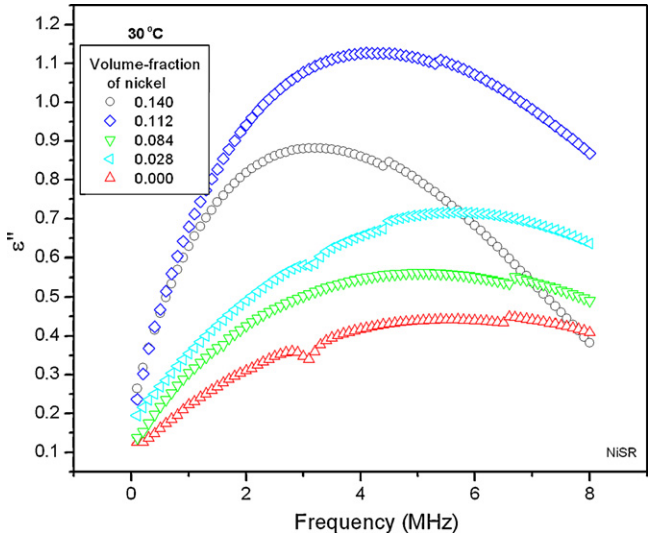

Fig. 11. Variation of dielectric loss of the composites with applied frequency at room temperature.

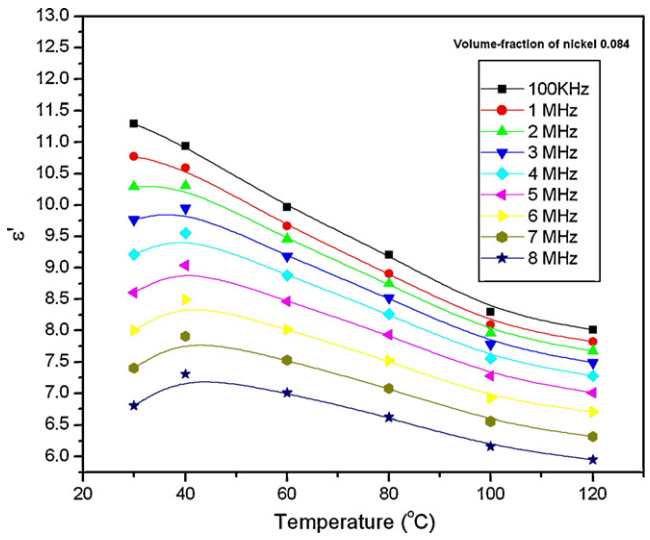

Fig. 12. Variation of dielectric permittivity with temperature at various frequencies of a 60 phr composite sample.

the dielectric permittivity increases in the temperature range of 30–40 °C and then decreases. This can be well understood on the basis of two competing factors influencing the dielectric behaviour of polymers [23]. One is the segmental mobility of the molecules of the polymer material and other is the differential thermal expansion of the elastomer matrix and the metal particles. The segmental mobility of the polymer material increases with temperature and this can enhance the polarization leading to an increase in the dielectric permittivity. But on the other hand, the differential thermal expansion, since the expansivity of neoprene ($6.1 \times 10^{-4}\,^{\circ}C^{-1}$) is greater than that of nickel ($3.9 \times 10^{-5}\,^{\circ}C^{-1}$), can aid the formation of metal clusters in the matrix causing a decrease in the area of the conducting filler and thereby causing a drop in the permittivity. There also exists a possible third reason in the form of the expansion of the neoprene matrix which can affect the measurement condition by the increase in the thickness of the neoprene disc resulting in a decrease in the measured capacitance. The enhanced segmental mobility appears to be predominant at lower temperatures up to 40 °C since the composites show an increase in permittivity and a decrease thereafter indicating the effects due to differential volume expansivity come into play after this temperature. Also it can be observed from the plots in Fig. 11 that this increasing and subsequent decreasing effect is totally absent in the frequency range up to 1 MHz suggesting that the segmental mobility is not much affected by the temperature at frequencies below 1 MHz and a rise in temperature enhances segmental mobility above this frequency which is a clear indication that the segmental mobility has a dependence on the applied frequency. Above 40 °C the formation of metallic clusters and volume expansivity of the matrix become more significant and result in a drop in permittivity.

4. Conclusion

Nickel–neoprene nanocomposites were prepared and were found to be homogeneous and agglomeration free. The evaluation of dielectric properties in the frequency range of 100 kHz to 8 MHz suggests that the dielectric properties can be tailored by an appropriate loading of the filler using a semi-empirical relationship. The magnetic properties of the composites can be tailored and predicted using simple mixture equations.

The dielectric permittivity increases with temperature initially (up to 40 °C) and it decreases afterwards. The segmental mobility of the matrix material comes into play in the initial stages and then the differential volume expansivity appears to become more effective in causing the decrease in the measured dielectric constant.

Acknowledgements

EMAJ acknowledges UGC (India) for the fellowship granted under faculty improvement programme. The authors acknowledge the financial supports from KSCSTE and AICTE.

References

[1] T. Tanaka, G.C. Montanari, R. Mulhaupt, IEEE Trans. Dielectr. Electr. Insul. II (5) (2004) 763–784.
[2] G.M. Tsangaris, G.C. Psarras, A.J. Kontopoulos, J. Non-Cryst. Solids 131–133 (1991) 1164–1168.
[3] G.C. Psarras, E. Manolakaki, G.M. Tsangaris, Composites A 33 (2002) 375–384.
[4] G.C. Psarras, Composites A 37 (2006) 1545–1553.
[5] P.S. Neelakanta, Handbook of Electromagnetic Materials, CRC Press, 1995.
[6] V. Singh, A.R. Kulkarni, T.R. Rama Mohan, J. Appl. Polym. Sci. 90 (2000) 3602–3608.
[7] M.R. Anantharaman, S. Sindhu, S. Jagatheesan, K.A. Malini, P. Kurian, J. Phys. D: Appl. Phys. 32 (15) (1999) 1801–1810.
[8] M. Morton, Rubber Technology, 3rd Ed., Van Nostrand Reinold Company, New York, 1995 (Chapter 12).
[9] K.H. Prema, Philip Kurian, P.A. Joy, M.R. Anantharaman, Polym. Plast. Technol. Eng. 47 (2008) 137–146.
[10] D. Rousselle, A. Berthault, O. Acher, J.P. Bouchaud, P.G. Zerah, J. Appl. Phys. 74 (1993) 475.
[11] Z.-M. Dang, C.-W. Nan, D. Xie, Y.-H. Zhang, S.C. Tjong, Appl. Phys. Lett. 85 (2004) 97–99.
[12] E.M.A. Jamal, P.A. Joy, P. Kurian, M.R. Anantharaman, Mater. Sci. Eng. B 156 (1–3) (2009) 24–31.
[13] H. Barron, Modern Synthetic Rubbers, Chapman and Hall, London, 1942, p. 322.
[14] R.D. Adams, J. Comyn, W.C. Wake, Structural Adhesive Joints in Engineering, 2nd Ed., Chapman & Hall, London, 1997, p. 192.
[15] E.M. Mohammed, M.R. Anantharaman, J. Instrum. Soc. India 32 (3) (2002) 165–171.
[16] H.V. Keer, Principles of Solid State Physics, Wiley Eastern Ltd., New Delhi, 1998.
[17] W. Gong, H. Li, Z. Zhao, J. Chen, J. Appl. Phys. 69 (1991) 5119.
[18] H.A. Pohl, Dielectrophoresis, Cambridge University Press, London, 1978.
[19] Derek C. Sinclair, T.B. Adams, F.D. Morrison, A.R. West, Appl. Phys. Lett. 80 (2002) 2153.
[20] B. Tareev, Physics of Dielectric Materials, MIR Publishers, Moscow, 1975.
[21] Y. Baziard, S. Breton, S. Toutain, A. Gourdenne, Eur. Polym. J. (24) (1988) 521.
[22] V.V. Daniel, Dielectric Relaxation, Academic Press, London, 1967.
[23] Z.M. Elimat, A.M. Zihilif, G. Ragosta, J. Phys. D: Appl. Phys. (41) (2008) 165408.